Low Temperature Physics/Fizika Nizkikh Temperatur, 2017, v. 43, No. 11, pp. 1575–1580

High-field magnetoelasticity of Tm_2Co_{17} and comparison with Er_2Co_{17}

A.V. Andreev[1], A.A. Zvyagin[2,3], Y. Skourski[4], S. Yasin[4,5], and S. Zherlitsyn[4]

[1]*Institute of Physics, Academy of Sciences, Na Slovance 2, Prague 182 21, Czech Republic*
E-mail: andreev@fzu.cz

[2]*B. Verkin Institute for Low Temperature Physics and Engineering of the National Academy of Sciences of Ukraine 47 Nauky Ave., Kharkiv 61103, Ukraine*

[3]*Max-Planck-Institut für Physik komplexer Systeme, 38 Nöthnitzrer Str., Dresden D-01187, Germany*

[4]*Dresden High Magnetic Field Laboratory, Helmholtz-Zentrum Dresden-Rossendorf, Dresden D-01314, Germany*

[5]*American University of the Middle East, College of Engineering and Technology, Egaila 54200, Kuwait*

Received February 24, 2017, published online September 25, 2017

Acoustic properties (ultrasound velocity and attenuation) and magnetostriction were measured in pulsed fields up to 60 T applied along the *c* axis of Tm_2Co_{17} single crystal. Similar to Er_2Co_{17}, the transition in Tm_2Co_{17} is accompanied by clear anomalies in the sound velocity. The observed 0.3% jump of the sound velocity at the transition is negative in Tm_2Co_{17}, whereas it is positive in Er_2Co_{17}. The magnetostriction at the transition also differs very much from that in Er_2Co_{17}. In Tm_2Co_{17}, the transition is accompanied by a smooth minimum of $0.15\cdot10^{-4}$ in longitudinal magnetostriction whereas in Er_2Co_{17} by a very sharp expansion of much larger magnitude ($1.2\cdot10^{-4}$). In the transverse mode, the effect in Tm_2Co_{17} looks as very broad minimum of low amplitude ($< 0.1\cdot10^{-4}$) whereas in Er_2Co_{17} as very sharp and large shrinkage ($2.6\cdot10^{-4}$). Thus, both the magnetoacoustics and magnetostriction are rather different in Tm_2Co_{17} and Er_2Co_{17}. This supports different nature of the field-induced transitions in these compounds.

PACS: **62.65.+k** Acoustical properties of solids;
75.47.Np Metals and alloys;
75.80.+q Magnetomechanical effects, magnetostriction.

Keywords: intermetallic compounds, magnetoelasticity, magnetostriction.

1. Introduction

Intermetallic compounds Tm_2Co_{17} and Er_2Co_{17} with the hexagonal crystal structure of the Th_2Ni_{17} type belong to the "2–17" series of R–T intermetallic compounds (R is a rare-earth and T is one of the late 3*d* transition metals — Fe, Co, Ni). The R–T intermetallics, especially with high content of the T metal, have been extensively studied for several decades because of their practical importance as high-performance magnetic materials. The magnetic behavior of the R sublattice is determined by the 4*f* electrons whereas the 3*d* electrons are responsible for the T-sublattice magnetism. The strongest exchange interaction is the 3*d*–3*d* interaction, which determines the high Curie temperature T_C. The exchange interaction between 4*f* electrons is very weak and can be neglected compared to other interactions. The 4*f*–3*d* interaction, although much weaker than the 3*d*–3*d* interaction, is of special importance since by this interaction the strongly anisotropic R-sublattice magnetization is coupled to the much less anisotropic T-sublattice magnetization. For this reason, some R–T compounds exhibit large anisotropy even at room temperature, what is basis for potential application of ferromagnetic R–T compounds (with light R) as permanent-magnet material.

In the R_2T_{17} compounds with heavy R elements (R = = Gd–Tm), the magnetic moments of the R and T sublattices are coupled ferrimagnetically. In high magnetic fields, this antiparallel structure will be broken and a forced-ferromagnetic state is expected. Transitions of this type have been found for the first time in Ho_2Co_{17} [1] and later in several other compounds (see for review Refs. 2–4).

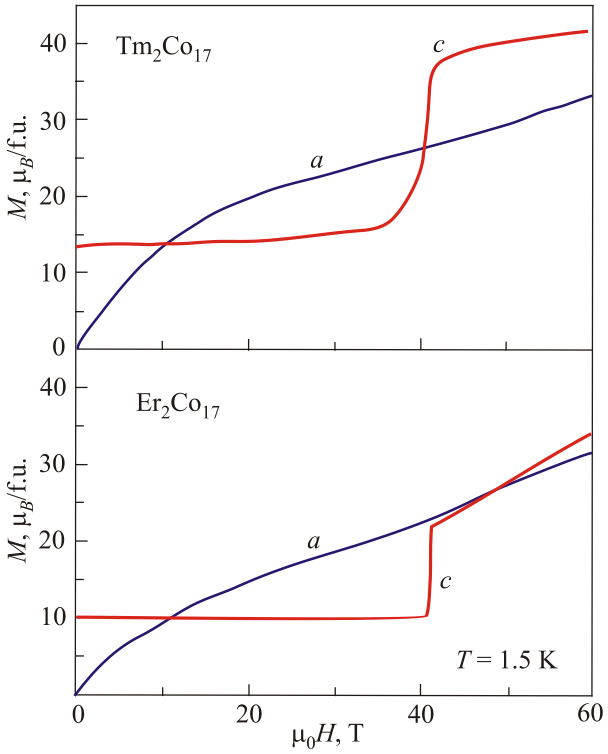

Fig. 1. (Color online) Magnetization curves of Tm_2Co_{17} and Er_2Co_{17} single crystals in field applied along the main axes at 1.5 K.

Since R_2T_{17} compounds exhibit large magnetic anisotropy, single crystals are strongly desirable for quantitative studies of their magnetism, and measurements of the magnetization and other properties related to the magnetism (e.g., magnetoelasticity) should be performed along the main crystallographic axes. Compounds Er_2Co_{17} and Tm_2Co_{17} where studied on single crystals in high magnetic fields in Refs. 5 and 6, respectively. They are ferrimagnets with rather similar magnetic properties. They have Curie temperature T_C = = 1170–1190 K, spontaneous magnetic moment M_S = 10 and 13.5 μ_B/f.u. for the Er and Tm compounds, respectively. In difference with all other R_2Co_{17} with heavy R having easy-plane type of magnetocrystalline anisotropy, Er_2Co_{17} and Tm_2Co_{17} have a large uniaxial anisotropy (Fig. 1). Anisotropy within the basal plane, very large in compounds R_2Co_{17} with easy-plane anisotropy (R = Tb, Dy, Ho), is negligible, for this reason only magnetization curves along the *a* axis are presented in Fig. 1. As seen in Fig. 1, both materials exhibit a field-induced transition in the vicinity of 40 T in a field applied along the *c* axis. In spite of the similar magnetic properties, the field-induced transitions in Er_2Co_{17} and Tm_2Co_{17} look different. In Ref. 6, we explained them as of completely different origins. In Er_2Co_{17} the transition is clearly of the first order and corresponds to sharp rotation of the Er sublattice by approx. 50 degrees with its further continuous alignment towards the collinear ferromagnet. Single Er^{3+} ion has magnetic moment 9 μ_B, so magnetic moment of the Er sublattice M_{Er} is 18 μ_B. Since $M_S = M_{Co} - M_{Er}$ = 10 μ_B, the Co-sublattice moment is 28 μ_B that corresponds well to M_S of R_2Co_{17} with nonmagnetic R = Y or Lu. Therefore, in forced ferromagnetic state $M_{ferro} = M_{Co} + M_{Er}$ = 46 μ_B. As it is seen in Fig. 1, the magnetic moment in 60 T, 34 μ_B, is still far from this value. As shown in Ref. 5, forced ferromagnetic state would be reached at about 70 T. In the case of Tm_2Co_{17}, the transition is attributed to a direct ferri-to-ferromagnetic transformation by way of paramagnetic remagnetization of the Tm sublattice. This is a continuous process, i.e., no intermediate canted-spin phases occur and the sublattice moments remain collinear with the applied field. One striking feature of the remagnetization process is that during its first stage, when $H < H_{cr}$, the magnetic field acts against the magnetic order in the Tm sublattice, driving the latter into a fully disordered state at $H = H_{cr}$ with further ordering in opposite direction, parallel to the Co sublattice. In Tm_2Co_{17}, where M_{Tm} = 14 μ_B, M_{Co} as $M_S + M_{Tm}$ = 27.5 μ_B. So, in the forced ferromagnetic state M_{ferro} = 41.5 μ_B. As seen from Fig. 1, $M(H)$ is almost saturated at 41 μ_B (in 60 T), very close to M_{ferro}.

The explanation of special high-field behavior of Tm_2Co_{17} given in Ref. 6 looks reasonable. Moreover, high-field magnetization study of the Fe analogue, Tm_2Fe_{17}, confirmed this model of the remagnetization process [7]. Nevertheless, it would be useful to confirm this by different behavior of other, in particular, magnetoelastic properties at the transitions in Er_2Co_{17} and Tm_2Co_{17}. The transition in Er_2Co_{17} is accompanied by pronounced anomalies in ultrasound velocity and magnetostriction [5]. We tried to measure these properties on the same crystal of Tm_2Co_{17} which was used for magnetization study in [6]. But that crystal occurred to be too small for the magnetoelastic measurements. Now we grew a new single crystal and prepared a 4×4×4 mm sample which is large enough for both acoustics and magnetostriction studies. Magnetization curves of previous and new crystals are the same, so there is no sample dependence.

In the present work we measured acoustic properties (ultrasound velocity and attenuation) and magnetostriction in pulsed fields up to 60 T applied along the *c* axis of Tm_2Co_{17} single crystal and compared them with results obtained for Er_2Co_{17}.

2. Experimental

A Tm_2Co_{17} single crystal was grown by a modified Czochralski method in a tri-arc furnace on copper water-cooled bottom from 7 g mixture of the pure elements (99.9% Tm, 99.99% Co). We used 1 at.% Tm excess to compensate its higher evaporation than that of Co. The pulling of crystal was performed under argon protecting atmosphere, a tungsten rod was used as a seed, at pulling speed 10 mm/h. The resulting single crystal was cylinder-shaped with a height of 20 mm and a diameter of 5 mm. Back-scattered Laue patterns confirmed the single-crystal-

line state of the sample. X-ray powder diffraction analysis confirmed single-phase state in the hexagonal crystal structure of the Th_2Ni_{17} type with lattice parameters a = = 828.6 pm, c = 809.4 pm in good agreement with those of crystal used in [6].

The magnetization curves were measured at 1.5–100 K in fields up to 60 T applied along the c axis using a pulsed-field magnet with pulse duration of 25 ms. A detailed description of the setup is given in [8]. Results of magnetization measurements, including field-induced transition, coincide with those of [6]. For the acoustic measurements, two piezoelectric film transducers were glued onto parallel polished facets perpendicular to the a axis of the crystal and the measurements were performed using a pulse-echo technique [9] at frequency 72 MHz. The magnetostriction was measured using an optical fiber strain gauge bonded to the surface of the sample with cyanoacrylate epoxy. The method is described in [10].

3. Results and discussion

Figure 2 presents results of magnetostriction measurements for Tm_2Co_{17} and Er_2Co_{17} at 1.5 K. Magnetic field is applied along the c axis (the field direction corresponds to the first index in linear magnetostrictions λ_{ca} and λ_{cc}, the second index is direction of the strain measurement). Since both compounds have uniaxial anisotropy, anisotropic magnetostriction constant, in particular, $\lambda_2^{\alpha,2}$, which reaches $-5.1\cdot10^{-4}$ and $-0.6\cdot10^{-4}$ in Tm_2Co_{17} and Er_2Co_{17}, respectively [11], does not contribute to the striction effect in this geometry (no striction is observed in low field during domain wall movement). Magnetostriction anomalies are seen in both compounds at field-induced transition. In Er_2Co_{17}, after an initial increase the linear magnetostriction exhibits a sharp stepwise anomaly. This applies to both the transverse magnetostriction λ_{ca} and the longitudinal one λ_{cc}. Along the c axis the lattice expands by $1.1\cdot10^{-4}$, whereas a contraction by $2.5\cdot10^{-4}$ is observed along the a axis. The geometry of the measurements is such that the results do not involve the magnetostriction constant λ^{γ} which describes the difference between the a and [120] axes in the basal plane. For this reason the volume effect can be evaluated as $\omega = 2\lambda_{ca} + \lambda_{cc}$. At the transition, a volume shrinkage of $\omega = -4\cdot10^{-4}$ is observed. As seen in Fig. 2, where results on Tm_2Co_{17} and Er_2Co_{17} are shown in the same, effects observed in Tm_2Co_{17} are much smaller. Moreover, the transition is not accompanied by transverse striction λ_{ca}.

Figure 3 shows longitudinal magnetostriction λ_{cc} of Tm_2Co_{17} at several temperatures in a larger scale, together with corresponding magnetization curves. One can see that at the transition the lattice not expands but shrinks along the c axis. The effect does not exceed by $-0.15\cdot10^{-4}$. The volume effect is equal to the same value due to zero transverse strain. The longitudinal effect is seen as clear anomaly at 20 K, as a very weak S-shape at 40 K and disappears at 60 K. It corresponds with strong temperature evolution

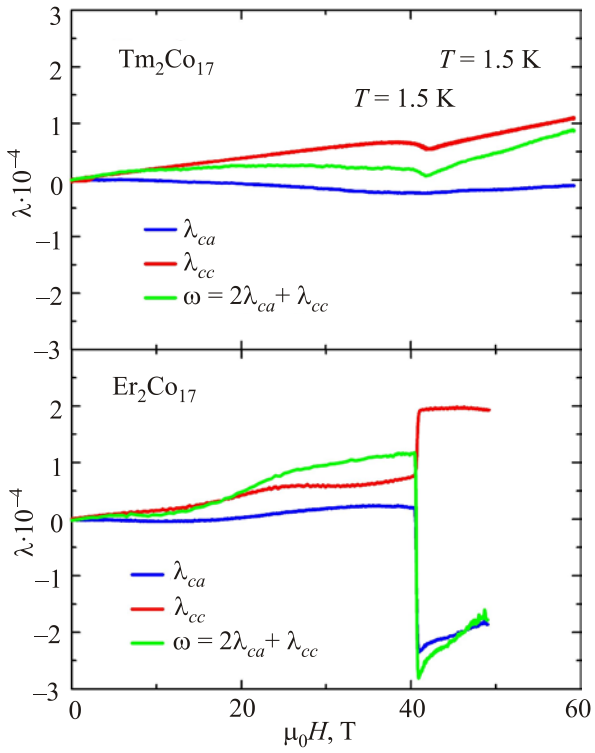

Fig. 2. (Color online) Field dependences of linear (λ_{ca}, λ_{cc}, the first index is the field direction, the second one is direction of length measurement) and volume magnetostriction ω in Tm_2Co_{17} and Er_2Co_{17} at 1.5 K.

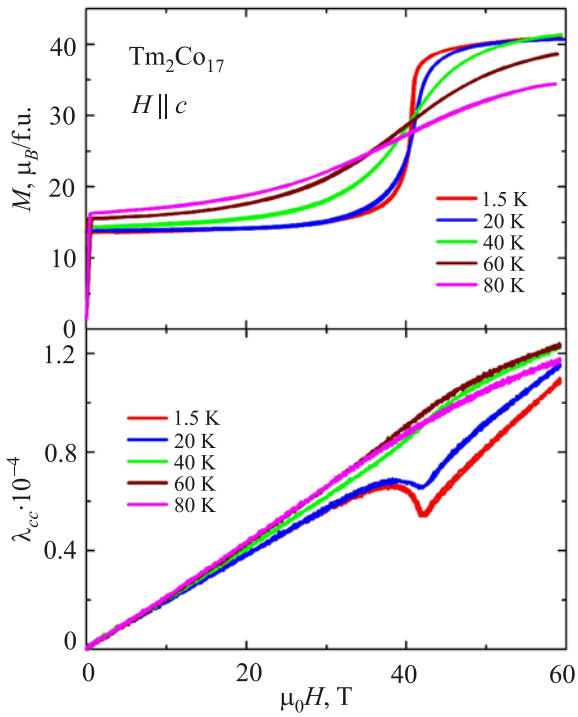

Fig. 3. (Color online) Temperature evolution of the magnetization curve along the c axis (upper panel) and longitudinal magnetostriction λ_{cc} in Tm_2Co_{17}.

of the magnetization curve. Thus, the results of magnetostriction measurements confirm our idea about different character of the field-induced transition in Tm_2Co_{17} and Er_2Co_{17} — magnetostriction effects are different quantitatively (by one order of magnitude) and qualitatively (different sign of λ_{cc}, absence of anomaly in λ_{ca} in Tm_2Co_{17}). The longitudinal effect is seen as clear anomaly at 20 K, as a very weak S-shape at 40 K and disappears at 60 K. It corresponds with strong temperature evolution of the magnetization curve (Fig. 3).

Field dependences of change of the ultrasound velocity $\Delta v/v$ in Tm_2Co_{17} and Er_2Co_{17} at several temperatures are shown in Fig. 4. Magnetic field is applied along the *c* axis, as well as sound propagation vector **k**. Sound polarization vector **u** is perpendicular to the *c* axis, so that it is transverse acoustic geometry. In both compounds the field-induced transition is accompanied by large acoustic anomaly, nevertheless, the effect has different sign, negative in Tm_2Co_{17} and positive in Er_2Co_{17}. In Tm_2Co_{17}, $\Delta v/v$ drops by $3\cdot10^{-3}$ whereas jump up by $4.5\cdot10^{-3}$ occurs in Er_2Co_{17}. Similar to the magnetostriction (Fig. 3), the anomaly vanishes at 60 K in the Tm compound. In Er_2Co_{17}, it is still seen at 60 K but at 80 K disappears as well. Figure 5 presents acoustic effect for longitudinal wave in Tm_2Co_{17}, when polarization vector **u** is parallel to the *c* axis together with propagation vector **k**. Results look similar to the transverse geometry, only the drop of $\Delta v/v$ is somewhat

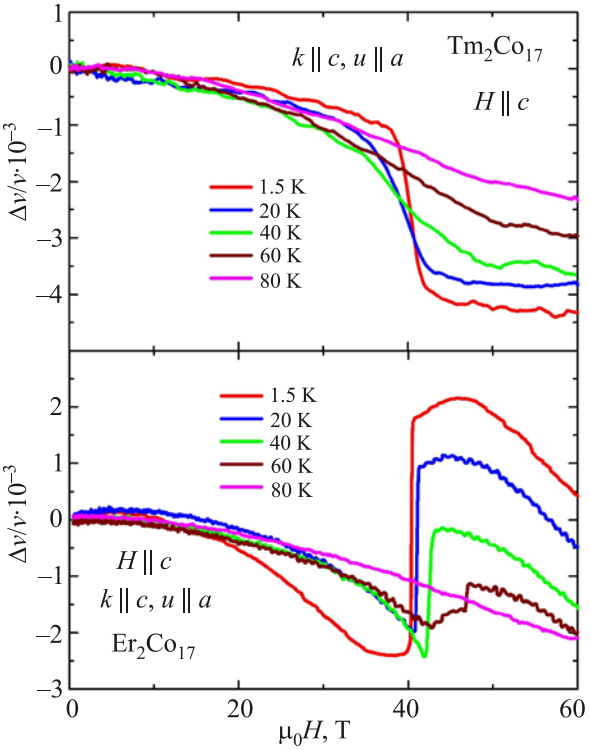

Fig. 4. (Color online) Field dependences of changes in the sound velocity of the wave along the *c* axis in transverse geometry ($k \parallel c$, $u \parallel a$) in Tm_2Co_{17} and Er_2Co_{17} at different temperatures.

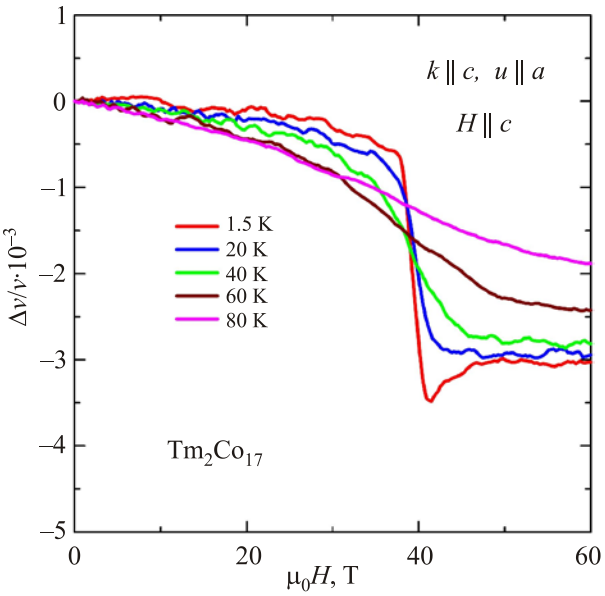

Fig. 5. (Color online) Field dependences of changes in the sound velocity of the wave along the *a* axis in the longitudinal geometry ($u \parallel a$) in Tm_2Co_{17} at several temperatures.

larger ($4\cdot10^{-3}$). The anomaly is also vanishes above 60 K. Another acoustic characteristic, sound attenuation $\Delta\alpha$, demonstrates very small anomaly at the field-induced transition in both compounds. Figure 6 shows field dependence of $\Delta\alpha$ in the transverse geometry, step at the transition does not exceed 2 dB/cm. Very similar curves were obtained in the longitudinal geometry (not shown).

The interaction between the elastic and magnetic degrees of freedom of magnetic systems is the reason of the renormalization of the sound characteristics. Usually, one

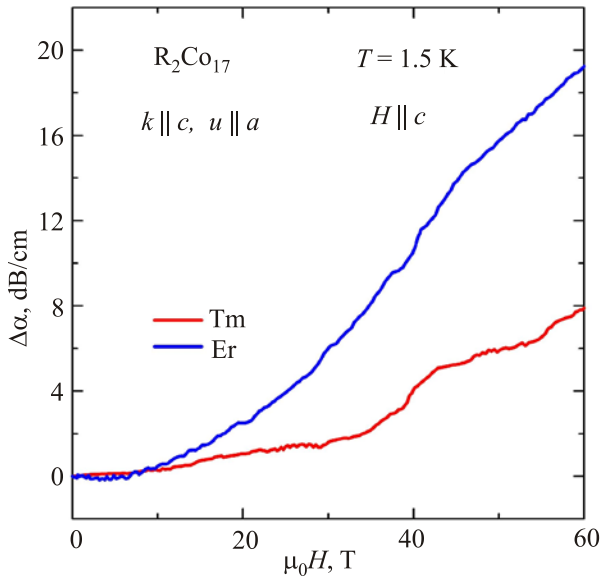

Fig. 6. Field dependences of changes in the sound attenuation of the wave along the *c* axis in the transverse geometry in Tm_2Co_{17} and Er_2Co_{17} at 1.5 K.

distinguishes between the contribution from the magnetic single-ion and inter-ion magnetic interactions. In the first case the main renormalization of the sound velocity comes due to the change of the position of the nonmagnetic ligands surrounding magnetic ions, caused by the sound wave. Such a change yields the change in the crystalline electric field, which, acting together with the spin-orbit coupling, changes the values of the effective g-factors and the parameters of the single-ion magnetic anisotropy. On the other hand, the main contribution from the inter-ion magnetic interactions is caused by the shifts of the positions of magnetic ions themselves, which produces the renormalization of magnetic interactions between magnetic ions (the exchange and magnetic dipole-dipole ones). In rare-earth compounds like Er_2Co_{17} and Tm_2Co_{17} both mechanisms contribute to the renormalization of the sound characteristics.

According to [12–16] the renormalization of the sound velocity v of the magnetic crystal can be written as

$$\Delta v/v \approx C_1[2M^2\chi_0 + k_BT\chi_0^2 + C_2(M^2 + k_BT\chi_0)],$$

where T is the temperature, M is the magnetization of the system, χ_0 is its homogeneous magnetic susceptibility (both of them depend on the temperature and external magnetic field H). When writing this expression, we neglect contributions from other components of the magnetic susceptibility and its inhomogeneity.

The constants C_1 and C_2 are determined as

$$C_1 = \frac{|g_0(\mathbf{k})|^2}{v^2\rho V(g\mu_B)^4 k_B^2}$$

and

$$C_2 = \frac{h_0(\mathbf{k})}{|g_0(\mathbf{k})|^2}\frac{(g\mu_B)^2}{4},$$

respectively. Here $\mathbf{k}$ is the wave vector of the acoustic phonon, ρ is the density of the crystal, V is the volume of the crystal, k_B is the Boltzmann constant, g is the g-factor, μ_B is the Bohr magneton,

$$g_0(\mathbf{k}) = \sum_j \left[\exp\left(i\mathbf{k}\mathbf{R}_{ji}\right) - 1\right]\mathbf{u}_k \frac{\partial J_{ij}}{\partial R_i},$$

$$h_0(\mathbf{k}) = \sum_j \left[-\cos\left(\mathbf{k}\mathbf{R}_{ji}\right) + 1\right]\mathbf{u}_\mathbf{k}\mathbf{u}_{-\mathbf{k}} \frac{\partial^2 J_{ij}}{\partial \mathbf{R}_i \partial \mathbf{R}_j}.$$

In the above formulas we denote by $\mathbf{u_k}$ the polarization of the sound wave, $\mathbf{R}_{ji} = \mathbf{R}_j - \mathbf{R}_i$, where $\mathbf{R}_i$ is the position vector of the ith site of the magnetic ion, and J_{ij} is the parameter of the effective interaction between the magnetic ions at sites i and j. Here we supposed that J_{ij} is determined by the contributions from inter-ion and single-ion magnetic interactions (which is reasonable for the studied rare-earth compounds). From the above we see that the temperature and the magnetic field dependence of the sound velocity are determined by the temperature and magnetic field dependence of the magnetization and the magnetic susceptibility of Er_2Co_{17} and Tm_2Co_{17}. The latter can be deduced from the experiment [5,6] and from the theory [6], which atisfactory described the magnetic field behavior of Tm_2Co_{17}.

Figure 7 shows the calculated magnetic field dependences of the renormalization of the transverse sound velocity for Tm_2Co_{17}. We used C_1 and C_2 as fitting parameters. Notice that we do not show the great renormalization of the sound velocity at zero field, caused by the spontaneous (partly) magnetized rare-earth ions [6]. We can see that for Tm_2Co_{17} the proposed theory describes the magnetic field behavior of the sound velocity rather good (compare with Fig. 4, upper panel). There is a step in the magnetic field dependence of the sound velocity at the critical field about $H_{cr} \sim 40$ T, which becomes smoother when the temperature grows. On the other hand, for Er_2Co_{17} there is a difference in the behavior of the calculated and the observed in experiments magnetic field behavior of the sound velocity. While the magnetic field behavior of the sound velocity for $H < H_{cr} \sim 40$ T is satisfactory, the predicted (absolute) value of the renormalization of the sound velocity for $H > H_{cr}$ is larger that the one, observed in the experiment for Er_2Co_{17}. It can be caused by the neglected in the theory contributions from the components of the magnetic susceptibility, perpendicular to the applied magnetic field, and from the inhomogeneous magnetic susceptibility. Our analysis implies, that despite similarity between chemical formulas for Er_2Co_{17} and Tm_2Co_{17} and the behavior of

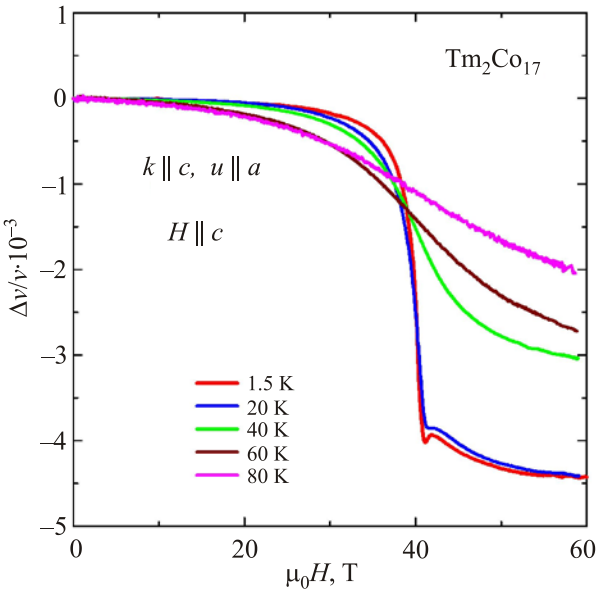

Fig. 7. (Color online) The calculated magnetic field dependences of changes in the transverse sound velocity in Tm_2Co_{17} at several temperatures.

their magnetizations, their magneto-elastic low-temperature properties are different. For Tm_2Co_{17} the main properties are mainly determined by the homogeneous component of the magnetic susceptibility, parallel to the direction of the external magnetic field. On the other hand, for Er_2Co_{17}, probably, for $H < H_{cr}$ the contributions from the components of the magnetic susceptibility, perpendicular to the applied external field, play the great role also.

Summary

Summarizing, we have studied experimentally the low-temperature magneto-elastic characteristics of the compound Tm_2Co_{17} in the external pulse mugnetic field up to 60 T. We have compared the magnetic and magnetoelastic features of the behavior of Tm_2Co_{17} and Er_2Co_{17}. Analyzing our results we see that both magnetoacoustics and magnetostriction characteristics behave rather differently for Tm_2Co_{17} and Er_2Co_{17}, supporting different nature of the field-induced transitions in these compounds. We can suppose that for Tm_2Co_{17} the main properties are determined by the homogeneous distribution of magnetic moments, while for Er_2Co_{17} magnetic moments can be distributed inhomogeneously. Also, in the region of field values lower than the critical one we can suppose that transverse (with respect to the direction of the field) components of the susceptibility of magnetic moments play the great role together with the longitudinal components, while in Tm_2Co_{17} mainly longitudinal components matter.

Acknowledgments

This work was supported by the Czech Science Foundation (project 16-03593S) and Materials Growth and Measurement Laboratory (http://mgml.eu/). We acknowledge the support of HLD at HZDR, member of the European Magnetic Field Laboratory (EMFL). A.A.Z. acknowledges the support from the DFG through SFB 1143 and the support from the Institute for Chemistry of the V.N. Karazin Kharkov National University.

1. J.J.M. Franse, F.R. de Boer, P.H. Frings, R. Gersdorf, A. Menovsky, F.A. Muller, R.J. Radwanski, and S. Sinnema, *Phys. Rev. B* **31**, 4347 (1985).
2. J.J.M. Franse and R. Radwanski, in *Handbook of Magnetic Materials*, K.H.J. Buschow (ed.), North Holland, Amsterdam (1993), Vol. 7, p. 307.
3. K. Kindo, M. Motokawa, and F.R. de Boer, in *High Magnetic Fields, Science and Technology*, F. Herlach and N. Miura (eds.) (2006), Vol. 3, p. 125.
4. K.H.J. Buschow, in *Handbook of Magnetic Materials*, K.H.J. Buschow (ed.), North Holland, Amsterdam (1997), Vol. 10, p. 463.
5. A.V. Andreev, Y. Skourski, M.D. Kuz'min, S. Yasin, S. Zherlitsyn, R. Daou, J. Wosnitza, A. Iwasa, A. Kondo, A. Matsuo, and K. Kindo, *Phys. Rev. B* **83**, 184422 (2011).
6. V. Andreev, M.D. Kuz'min, Y. Narumi, Y. Skourski, N.V. Kudrevatykh, K. Kindo, F.R. de Boer, and J. Wosnitza, *Phys. Rev. B* **81**, 134429 (2010).
7. O. Isnard, A.V. Andreev, M.D. Kuz'min, Y. Skourski, D.I. Gorbunov, J. Wosnitza, N.V. Kudrevatykh, A. Iwasa, A. Kondo, A. Matsuo, and K. Kindo, *Phys. Rev. B* **88**, 174406 (2013).
8. Y. Skourski, M.D. Kuz'min, K.P. Skokov, A.V. Andreev, and J. Wosnitza, *Phys. Rev. B* **83**, 214420 (2011).
9. B. Wolf, B. Lüthi, S. Schmidt, H. Schwenk, M. Sieling, S. Zherlitsyn, and I. Kouroudis, *Physica B* **294–295**, 612 (2001).
10. R. Daou, F. Weickert, M. Nicklas, F. Steglich, A. Haase, and M. Doerr, *Rev. Sci. Instrum.* **81**, 033909 (2010).
11. A.V. Deryagin, N.V. Kudrevatykh, R.Z. Levitin, and Y.F. Popov, *Phys. Status Solidi* (a) **51**, K125 (1979).
12. M. Tachiki and S. Maekawa, *Progr. Theor. Phys.* **51**, 1 (1974).
13. O. Chiatti, A. Sytcheva, J. Wosnitza, S. Zherlitsyn, A.A. Zvyagin, V.S. Zapf, M. Jaime, and A. Paduan-Filho, *Phys. Rev. B* **78**, 094406 (2008).
14. S. Yasin, A.V. Andreev, Y. Skourski, J. Wosnitza, S. Zherlitsyn, and A.A. Zvyagin, *Phys. Rev. B* **83**, 134401 (2011).
15. A.A. Zvyagin, S. Yasin, Y. Skourski, A.V. Andreev, S. Zherlitsyn and J. Woznitsa, *J. Alloys Comp*. **528**, 51 (2012).
16. A.V. Andreev, S. Yasin, Y. Skourski, A.A. Zvyagin, S. Zherlitsyn, and J. Wosnitza, *Phys. Rev. B* **87**, 214409 (2013).